

## **A Method for Comparison of Cadaveric Human Head Masses, Centers of Gravity and Moments of Inertia: Direct Measurement vs. Computed Tomographic Calculation**

C. B. Albery, J. J. Whitestone, C. E. Perry,  
D. D. Wilson, G. C. Raynak, R. P. Ching

### **ABSTRACT**

*Mass properties of the human head are critical elements in developing neck injury threshold criteria in acceleration and impact environments. In order to accurately simulate the dynamics of the head in impact and acceleration environments, valid mass properties data for the human head must exist. The purpose of this study was two-fold: first, to investigate the potential for using computed tomographic (CT) analyses to calculate the inertial properties of the human head and second, to directly measure and generate a useful data set of human head mass properties and anthropometry. Fifteen cadaveric human heads, 8 male and 7 female, were measured. Approximately 35 anatomical features on the head were digitized and a head anatomical coordinate system was defined. For the direct measurement procedure, each frozen specimen was secured in a lightweight-aluminum box. The mass, center of gravity (CG) and moments of inertia (MOI) were then measured. These same properties of the box alone were subtracted from the measured quantities to determine each specimen's mass properties. For the CT analysis, the identical specimen preparation was imaged with CT. With both slice collimation and table feed set at 1mm, the CT image resolution was 0.284 mm<sup>3</sup>/voxel. Segmentation of tissue types based on density thresholds was used to divide the volumetric data into brain matter, bone, and fat/skin. Surfaces from these groups were extracted to create volumes representing these structures. Assigning mass densities to the segmented volumes, the mass properties of the head were calculated using Computer-Assisted Design (CAD) calculations for comparison to the directly measured mass properties.*

### **INTRODUCTION**

**T**he human body's response to excessive accelerations and impact is largely dependent on the body's inertial properties and any encumbering equipment. Without doubt, the head and neck are among the most exposed elements of the body in these harsh dynamic environments. This issue has

been recognized by the government and within the medical and commercial communities for several decades. A great deal of research has been performed on characterizing the inertial properties of the heads and necks of cadavers and living humans (Harless, 1860; Clauser, McConville, Young, 1969; Becker 1972; Walker, Harris, Pontius, 1973; Chandler, Clauser, McConville, Reynolds, Young, 1974; Beier, Schuller, Schuck, Ewing, Becker, Thomas, 1980; McConville, Churchill, Kaleps, Clauser, Cuzzi, 1980; Kaleps, Clauser, Young, Zehner, McConville, 1984).

Within the United States Air Force, devices that encumber the head and neck often include helmets, oxygen masks, and helmet-mounted optics, especially for an aircrew member. The mass properties and the mass distribution of these devices relative to the head are critical design parameters for helmets and head-supported equipment. These parameters could affect the comfort, fit, performance and crash or ejection safety of head-mounted equipment. The distribution of head-supported mass could also affect the fatigue experienced by aircrew members. The mass properties parameters which have been identified as most important when designing helmet systems are total head-supported mass, moments of inertia (MOI), and the center of gravity (CG) location of the head-supported equipment (Knox, Buhrman, Perry, 1992; Self, Spittle, Kaleps, Albery, 1992; Whitestone, Albery, 1996). Likewise, for advanced computations and accurate dynamic modeling, it is essential to have a prior knowledge of the mass properties of these equipment simulated in the model (Schultz, Obergefell, Rizer, Albery, Anderson, 1997; Beier et al., 1980).

## BACKGROUND

This research was made possible due to a Cooperative Research and Development Agreement (CRADA) between the US Air Force Research Laboratory's Biodynamics and Acceleration Branch (AFRL/HEPA) and the University of Washington's Orthopaedic & Biomechanics Lab (UW-OBL). One of the primary missions of the AFRL/HEPA is to conduct experimental research to define the human response to transient biodynamic stresses such as impact acceleration and aerodynamic forces. With the goal of developing aeromedical injury tolerance criteria, it is essential to understand the envelope of dynamic stresses within which the human body can operate without injury. Towards establishing these criteria, the experimental research often includes the exposures of human volunteers to a defined range of acceleration pulses. In order to accurately develop these criteria, and successfully model the head and neck reaction to these pulses, it is important to have an accurate record of the mass properties of volunteer-subjects' head. Since it is impossible to directly measure the subjects' head mass properties accurately without segmentation, it would be very helpful to develop a method for computing the head mass properties of the living human. Hence, the current studies were conducted to investigate the potential for using computed tomography (CT) analysis to accurately calculate the inertial properties of the living human head. Another application of this methodology that would benefit is custom-fit and ballasted helmets to lessen the risk of increased bending and rotational moments due to an offset of the current head CG.

Due to recent advancements in medical imaging, we can now provide three-dimensional representations of CT data. Live human heads can now be volume rendered. Segmentation of tissue types including brain matter, fat, bone, and skin will allow for a morphological map of the head to which mass densities can be assigned. Assuming that a relationship exists between Hounsfield Units (a normalized index of x-ray attenuation used in CT imaging based on a scale of -1000 (air) to +1000 (bone), with water being 0), and physical density, each voxel (a contraction for volume element that is the base unit for CT reconstruction; represented as a pixel in the display of the CT image) representing the object can be assigned a physical density. These segmented volumes can then be used to determine mass properties of the whole head.

To determine the reliability of using electronic imaging to determine mass properties, a commercial mass properties measurement system with known accuracy (Self et al., 1992) can be used to directly measure and validate the imaging results. Our immediate objective was to develop a methodology to directly measure the mass, CG, and MOIs of cadaveric human head specimens, and to develop the methodology for calculating the inertial properties of these specimens using CT analyses. Once these methodologies are proven accurate and reliable, the ultimate goal of verifying the efficacy for using CT analysis to accurately calculate the inertial properties of the living human head will be completed. This will lead to the development of a useful database of human head mass properties and anthropometry. The results of these two procedures will provide human head mass properties data, both measured and calculated, with respect to a head anatomical coordinate system. This common coordinate system allows for comparison of the two methods of data collection. At the time this study was presented, these methodologies were still being developed and utilized. Therefore, the focus of this paper will concentrate on the current methodology used to collect these data. A summary of the measured mass properties data are presented.

## METHODS

### Specimens

Eight male and seven female cadaver specimens were measured. The male specimens ranged in age from 16-80 years at time of death, with a mean age of  $55 \pm 22$ . The female specimens ranged in age from 23-97 years at time of death, with a mean age of  $62 \pm 24$ . Overall (both male and female), the specimens ranged in age from 16-97 years at time of death, with a mean age of  $59 \pm 22$ .

All specimens were acquired from the International Institute for the Advancement of Medicine (IIAM), Scranton, PA. Before delivery, all specimens were scanned for blood-borne pathogens, such as hepatitis and HIV. The specimens were ordered and received with at least the neck (cervical spine) still attached to the head. The necks were used in another concurrent study. Therefore, in order for the specimens to be considered, they had to have no history of head or neck trauma. The head and neck specimens were radiographed for gross degenerative changes or abnormalities and visually inspected for confounding pathologies. Any specimens not meeting our requirements were rejected. All specimens were handled according to Center for Disease Control (CDC) guidelines upon delivery. All specimens remained frozen ( $-20^{\circ}\text{C}$ ) until they were used in the study, at which time they were thawed according to the requirements for that particular part of the study. All specimens were naturally drained, and were not flushed nor embalmed.

### Mass Properties: Direct Measurement

*Procedural overview.* The procedure consists of measuring the combined mass, CG, and MOIs of a specimen secured within a support box and then measuring the properties of the support box by itself. The contribution from the support box is then subtracted from the combination, resulting in the mass, CG, and MOIs of the specimen alone. All predetermined landmarks on the head were then digitized in order to generate a head anatomical coordinate system and to acquire the data necessary to calculate various anthropometry. The specimens' CG location was calculated with respect to a head anatomical axis system. The head anatomical axis system was used to locate the position of the specimens' CG with respect to the head and was defined by anatomical landmarks on the surface of the head and face. The principal MOIs were defined at the specimens' CG location. In addition, basic anthropometric measures were recorded, such as head circumference, head breadth, and head length.

*Equipment.* The direct measurement procedure included a three-sided orthogonal support box

to secure the specimen during testing; a digital balance and moment table to determine the mass and CG; an MOI instrument to record the specimens' principal MOIs; a three-dimensional digitizer to determine the anatomical coordinate system and location of the predetermined anatomical landmarks; anthropometric tools, such as ribbon tape, and calipers to perform basic anthropometry; and a computer for data acquisition and analysis.

*Marking the anatomical features.* The first step was to thaw the specimen until the skin was palpable. The specimen was then shaved, cleaned and dried. Approximately 35 predetermined anatomical features were located by palpating the flesh and marked with permanent ink (FIG. 1). Lead markers, called Beekley® spots, commonly used in radiographs, were placed on key landmarks and were used to set up the specimen's head anatomical coordinate system. The landmarks identified, marked and recorded were chosen either to satisfy the requirements for generating the anatomical coordinate system or to determine physical anthropometric dimensions; for comparison to previous studies. Some of the landmarks not shown on FIG. 1 include the apex, occiput, nuchale, and occipital condyles, as well as three reference landmarks on the forehead.

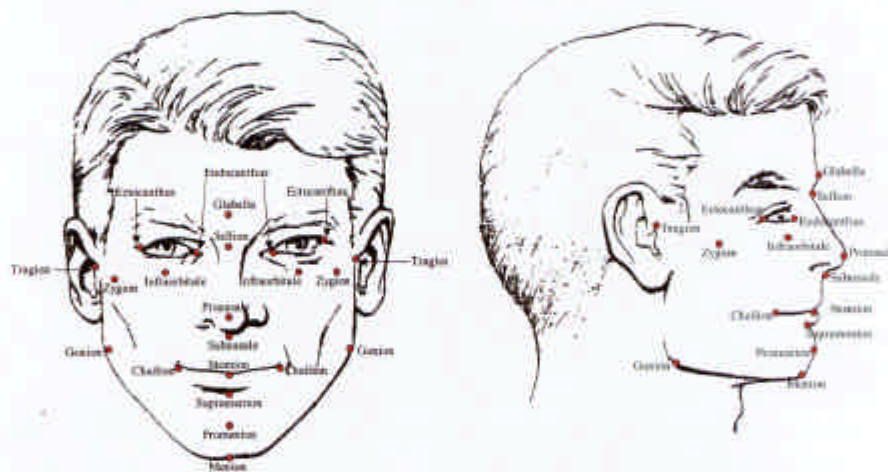


FIG. 1. Anatomical Features Recorded

*The head anatomical coordinate system.* This system is based on the Frankfort plane of the Head. Locating, marking with the Beekley® spots and digitizing four key landmarks generates this plane. The Y axis of the head anatomical coordinate system (positive to the left) is generated by digitizing the left and right tragions, located at the notch just above the tragus of the left and right ear. A vector from the right infraorbitale normal to the Y axis establishes the X axis of the head anatomical coordinate system (positive toward the front). The infraorbitale is located at the lowest point on the inferior margin of the orbit of the right eyesocket. The origin of the head anatomical coordinate system is at the intersection of these axes with the Z axis positive upward. The coordinate system is finally translated to the mid-sagittal plane of the head by digitizing the sellion (located at the greatest indentation of the nasal root depression (FIG. 2).

*Dissection of the neck from the head.* The head and neck went through a three-step dissection technique. This multi-phase technique was necessary due to the concurrent neck research. A portion of the head had to remain intact (attached to the neck) until the neck testing was complete. This segmentation included a posterior-to-anterior cut from the occipital protuberance to the zygomatic

process and sphenoid bone (FIG. 3a). Then an inferior-to-superior cut completed the initial segmentation (FIG. 3B). Upon completion of the neck testing, the portion of the skull was reattached using adhesive (FIG. 3C). The final segmentation was performed utilizing a technique much like that of past cadaveric head mass properties studies (Walker et al., 1973; Beier et al., 1980). This cut originates just below the external occipital protuberance, proceeding anteriorly and inferiorly to the atlantooccipital joint, then onto prevertebral muscle mass, intersecting with a cut just superior to the hyoid bone that extends cranially and posteriorly (FIG. 3D).

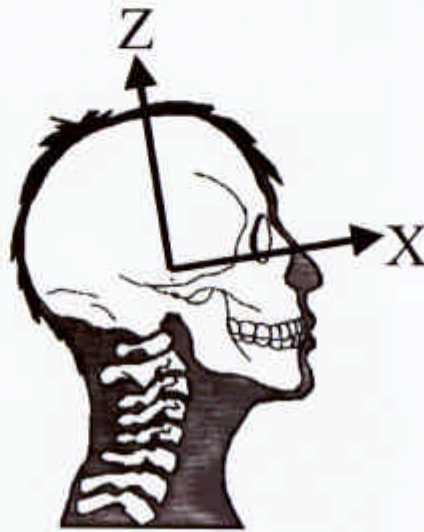


FIG. 2. Head Anatomical Coordinate System

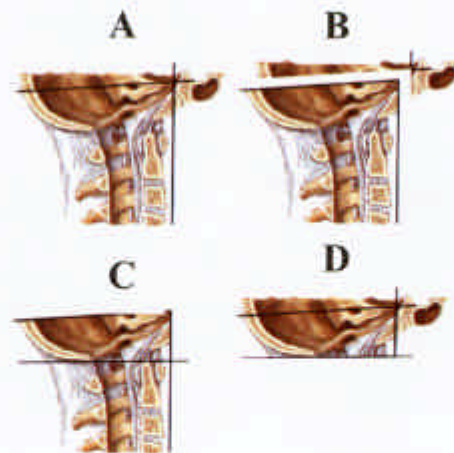


FIG. 3. (A & B) Initial dissection of the head from the neck to allow a portion of the skull to remain attached to the neck for the concurrent neck study. (C) Reattachment of the portion of the skull. (D) Final segmentation separates the head and neck.

*Securing the head within the support box.* In order to directly measure the mass properties, the specimen was first mounted in a lightweight orthogonal support box. The three sides of the support box form mutually perpendicular planes that form the X, Y and Z axes with the corner designated as the origin. Hook and loop straps or strips of tape were used to hold the specimen tightly within the box. The box properties are predetermined and later subtracted, leaving just the specimen properties. The box not only serves as a means for fixing the specimen during testing, it also serves as a source from which all the data are initially referenced.

*Mass and CG determination.* The mass of the specimen was determined by placing the specimen and support box on an electronic balance and recording the mass (FIG. 4).

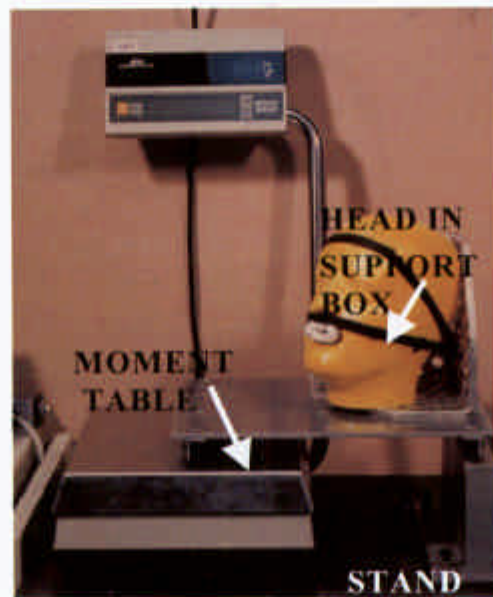


FIG. 4. Manikin Head within the Support Box being Measured for  $CG_x$

The CG location is determined with the use of the balance and a moment table assembly. The moment table is an aluminum plate supported by two steel knife-edge blades with their edges parallel to each other and separated by a known distance. An aluminum chock is secured to the top of the plate directly above one of the steel blades. During testing, the chock side of the table is placed on an adjustable stand and the other side is placed on the electronic balance. The stand is adjusted until the table is level and then the balance is zeroed. The force of the first moment of the specimen within the box along each axis is determined directly from the balance reading. With the mass of the specimen within the box as well as the blade-to-blade horizontal separation distance, the position of the composite center of mass is calculated using summation of moments about the chock edge and results in

$$X_{CG} = \frac{F_S R_S}{F_{CG}}$$

where  $F_S$  = Balance reading of specimen within the support box on the moment table (converted to weight)

$F_{CG}$  = Weight of the specimen within the support box

$R_S$  = Known moment arm blade separation distance

$X_{CG}$  = CG coordinate of specimen within the support box with respect to the support box in contact with the chock.

To determine the CG of the specimen alone, the entire procedure was repeated for the empty support box. The empty support box CG was then subtracted from the combined specimen and box data, resulting in the CG of the specimen. Since first moments are additive, the center of mass of the specimen with respect to the support box axis system is determined by subtracting the support box contribution:

$$X_T = \frac{F_{CG} X_{CG} - F_B X_B}{F_T}$$

where  $F_T$  = Weight of the specimen

$F_{CG}$  = Weight of the specimen within the support box

$F_B$  = Weight of the support box

$X_T$  = X axis CG location of the specimen

$X_{CG}$  = X axis CG location of the specimen within the support box

$X_B$  = X axis CG location of the support box.

This procedure is repeated for the Y and Z axis CG locations.

Once the CG is calculated, the moments about the combined CG of the specimen and box can be measured.

*Moments of Inertia Determination.* Specimen MOIs were measured with the specimen secured in the support box and placed on a XR-50 Space Electronics Mass Properties Instrument. The instrument measures the MOIs about a torsional pendulum axis. The moment measured was that of the pendulum itself, plus the pendulum platform, and the specimen within the box upon the pendulum platform. The pendulum platform consisted of a 1' x 1' x .25" honeycomb gridded platter. This platter is marked in 0.1 in. increments to ensure accurate placement of the specimen within the box.

This instrument functions most accurately when the CG position of the object being tested is initially aligned with the fixed pendulum axis. Therefore, the standard procedure was to mount the specimen within the box on the gridded test platter with the horizontal CG position of the composite within +/-0.01 in. of the pendulum's vertical axis. Once the specimen within the box was in place, the MOI measurement was recorded. This process was repeated for all six MOIs, with the specimen within the box being reoriented between each measurement.

When the platter, given an angular displacement,  $\theta$ , from its equilibrium position, is triggered, it oscillates due to the restoring torque,  $T$ , exerted by the instrument's shaft. The magnitude of  $T$  is given by

$$T = \frac{GJ}{L} \theta = K_t \theta$$

where  $K_t$  is the torsional spring constant of the shaft and is a function of the shear modulus,  $G$ , the length of the shaft,  $L$ , and the polar moment of inertia,  $J$ , of the cross section of the shaft.

If the torsional moment of inertia of the platter is  $I$  and the torsional force acts to bring the

system back to equilibrium, then we can write

$$-K_t \theta = I \frac{d^2 \theta}{dt^2}$$

This equation can also be written as

$$\frac{d^2 \theta}{dt^2} + \frac{K_t}{I} \theta = 0$$

that is a homogenous differential equation for which the solution is

$$\theta = C_1 \cos \sqrt{\frac{K_t}{I}} t + C_2 \sin \sqrt{\frac{K_t}{I}} t$$

where  $C_1$  and  $C_2$  are constants which can be determined from the initial conditions. If the initial conditions are

$$\theta \text{ at } t = 0 \text{ equals } 0$$

and

$$\theta \text{ at } t = \frac{\pi}{2} \sqrt{\frac{I}{K_t}} \text{ equals } A$$

then  $C_1 = 0$ , and  $C_2 = A$  and the previous equation becomes

$$\theta = A \sin \sqrt{\frac{K_t}{I}} t$$

This is the equation for simple harmonic motion that  $\sqrt{\frac{K_t}{I}}$  is the angular frequency,  $\omega_n$ , at which the platter and shaft oscillate in radians per second. The period of oscillation,  $\tau_n$ , is given by

$$\tau_n = \frac{1}{\omega_n} = \sqrt{\frac{I}{K_t}}$$

Solving this equation for the moment of inertia gives

$$I = K_t \tau_n^2$$

The rotational inertial properties of the specimen within the box can be expressed by an inertia tensor. The tensor values depend on the coordinate system origin and orientation with respect to the tensor being calculated. Moment of inertia measurements were taken about six different axes to generate an inertia tensor from which the orientation of the principal axes and the magnitudes of the principal MOI were determined. For simplicity, three of the axes chosen (X, Y, Z) were about the cardinal axes (both edges) of the support box. Figure 5 shows specimen being measured about one of the cardinal axes. The remaining three axes (XY, YZ, XZ) were axes in the planes of the three walls of the support box at 45-degree angles to the cardinal axes. These 45-degree measurements were taken using a custom-made lightweight jig, as shown in FIG. 6. All six axes intersect at the origin of the box's coordinate system.



FIG. 5. Manikan head within the support box being measured for MOI about a cardinal axis



FIG. 6. Manikan head within the support box being measured for MOI about a noncardinal axis

From the six moment measurements, the products of inertia or diagonal elements of the inertia tensor can be determined from the equation

$$P_{ab} = \frac{I_a + I_b \tan^2 \theta - (1 + \tan^2 \theta) I_{ab}}{2 \tan \theta}$$

where  $P_{ab}$  = the product of inertia in the ab plane  
 $I_a$  = the moment of inertia about the cardinal axis a  
 $I_b$  = the moment of inertia about the cardinal axis b  
 $I_{ab}$  = the moment of inertia about the noncardinal axis in the ab plane  
 $\theta$  = the angle between axis a and axis b.

Because the angle between axes is  $45^\circ$ , the equation simplifies to

$$P_{ab} = \frac{I_a + I_b - 2I_{ab}}{2}$$

Upon completion of the six moment measurements with the specimen within the box, the entire procedure was repeated with the empty box. The box plus jig inertial properties were subtracted from the measured composite properties using the parallel axis theorem.

The resulting inertia tensor, which was with respect to the center of mass of the test object, can be written as

$$\underline{I} = \begin{bmatrix} I_x & -P_{xy} & -P_{xz} \\ -P_{yx} & I_y & -P_{yz} \\ -P_{zx} & -P_{zy} & I_z \end{bmatrix}$$

This inertia tensor is symmetric and can be reduced to diagonal form in which the products equal zero and the diagonal elements are the principal moments. This is accomplished by determining the values of  $\lambda$  which satisfy the equation

$$(\underline{I} - I\lambda)\omega = 0$$

where  $I$  are the principal moments of inertia. The vectors associated with these values are the

directions of the principal axes associated with the principal moments of inertia. These vectors, expressed as a matrix of cosines, define the directions of the principal axes with respect to the axis parallel to the box axis system, but are centered at the specimen CG.

*Coordinate System Transformation.* To this point, all measurements were located with respect to the box coordinate axes. To reference the properties of the specimen to a head anatomical coordinate system, the specimen landmarks were digitized with respect to the box coordinate system (box edges) using the electronic position coordinate digitizer. The box origin, located at the rear and right-hand corner of the outer box, and points representing the X, Y, and Z axes of the box (box edges) were digitized along with all the pre-marked head and face landmarks (FIG. 7). Those points not accessible due to the frame of the box were digitized upon removal of the box along with at least three points from the previous set, thus allowing for inclusion in the final data set.

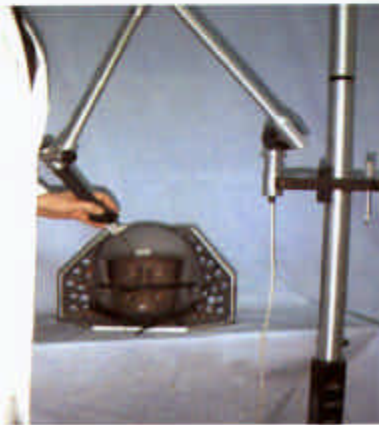


FIG. 7. Manikan head and Helmet within Support box being Digitized

### **Mass Properties: Computed Tomography (CT) Protocol**

*Overview.* Fifteen unembalmed cadaver heads were used for estimating mass properties. The spiral CT data were collected by the University of Washington's Orthopaedic & Biomechanics Lab, located at the Harborview Medical Center, Seattle, WA. These data were transferred electronically to Total Contact Inc., Dayton, OH for segmentation and determination of mass properties.

*CT imaging.* The CT imager used was the GE High Speed Advantage System. This system has an X-Ray strength of 120kV at 80mA. With both slice collimation (thickness) and table feed set at 1 mm, the following are the resultant dimensional resolutions:

- 1-D resolution = 273 mm circle at 512 pixels = 0.5332 mm/pixel
- 2-D resolution = 273 mm x 273 mm at 512 pixels x 512 pixels = 0.2843 mm<sup>2</sup>/pixel<sup>2</sup>
- 3-D resolution = 273 mm x 273 mm x 1 mm at 512 pixels x 512 pixels x 1 pixel = 0.2843 mm<sup>3</sup>/pixel<sup>3</sup> = 0.2843 mm<sup>3</sup>/voxel



FIG. 8. Slice of spiral CT data with Beekley® spot and phantom

Figure 8 shows an example slice of spiral CT data. The image is represented as a gray scale image and shows the 2-D view of the head. Likewise, the image shows the density phantom (product information) Beekley® spot, as well as the bone, brain, and soft tissue. Contrary to this image, all scans were performed with the head in the prone position and progressed caudad.

*Segmentation and calculation of mass properties.* Tissue segmentation was performed using Analyze AVW as shown in FIG. 9. This biomedical visualization and analysis software was developed over the last 10 years for the Mayo Clinic by a team of physicians, biomedical engineers, and programmers. This program contains advanced automated segmentation routines including thresholding, 2-D and 3-D region growing, automated boundary detection, and morphological processing. The resulting Hounsfield Units were used to categorize each voxel into brain, CSF, fat, bone, and skin. Surfaces from these groups were extracted to create volumes representing these structures. The surfaces were transferred to AutoCAD or a similar CAD package for calculating the whole head mass, CG, and principal MOIs (Whitstone, 2000).



FIG. 9. Example of Analyze AVW visualization and analysis capability

Figures 10A and 10B show the segmented soft tissue (skin) and bone (skull) as extracted from the spiral CT data using Analyze AVW. Likewise, in Figures 10C and 10D the skull is visualized with the brain. This image was also segmented from the spiral CT data. This exercise demonstrates the ability to segment 2-D CT data slices resulting in 3-D surface representations of various tissue types.

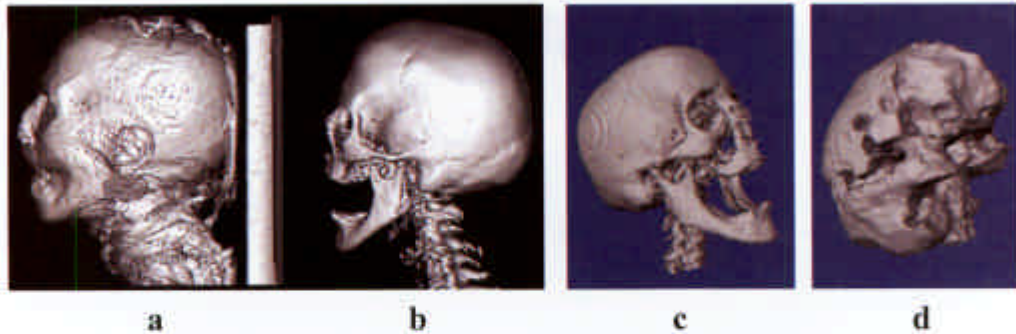


FIG. 10. Segmented soft tissue/skin (A) and bone/skull (B). Segmented bone/skull (C) and brain (D). All images were extracted from the spiral CT data using Analyze AVW.

## RESULTS

### Mass Properties: Direct Measurement

*Data tables.* Three data tables list the measured mass properties for the female specimens (Table 1), male specimens (Table 2), and a summary for all specimens (Table 3).

A comparison of the mean values for gender of each recorded measure (mass,  $CG_X$ ,  $CG_Y$ ,  $CG_Z$ ,  $MOI_X$ ,  $MOI_Y$ ,  $MOI_Z$ ) was performed. All comparisons were performed at a significance level of  $\alpha = .05$ .

If the variances of the males and females were found to be not significantly different, then a 2-sample, 2-tailed t-test was performed. Using this statistic, no significant difference was determined for  $CG_X$  {T (13) = 0.59,  $p = 0.5624$ },  $CG_Y$  {T (13) = 0.17,  $p = 0.8668$ }, and  $CG_Z$  {T (13) = 0.82,  $p = 0.4283$ }. Conversely, using this statistic, a significant difference was determined for  $MOI_X$  {T (13) = 3.40,  $p = 0.0048$ }.

If the variances of the males and females were found to be significantly different, then an approximate, 2-tailed t-test was performed using Satterthwaite's approximation for degrees of freedom. Using this statistic, a significant difference was determined for the **mass** {T (7.8) = 3.59,  $p = 0.0074$ },  $MOI_Y$  {T (8.1) = 3.84,  $p = 0.0048$ }, and  $MOI_Z$  {T (9.3) = 2.55,  $p = 0.0305$ }.

These statistics indicate that a significant gender difference was found for mass, and the principal moments of inertia, but not for the centers of gravity.

When the calculated mass properties results become available from the CT imaging analysis, they will be compared to the results shown above. Likewise, these data will be compared to the past studies referenced earlier in this paper.

Table 1: Female Specimen Mass Properties

Female Specimens	Mass (kg)	CG <sub>x</sub> (cm)	CG <sub>y</sub> (cm)	CG <sub>z</sub> (cm)	MOI <sub>x</sub> (kg-cm <sup>2</sup> )	MOI <sub>y</sub> (kg-cm <sup>2</sup> )	MOI <sub>z</sub> (kg-cm <sup>2</sup> )
S/N F02	2.98	-0.19	0.48	2.55	83.98	128.16	124.94
S/N F05	2.78	-0.34	0.58	2.86	74.61	112.07	107.97
S/N F06	3.00	0.42	-0.58	2.18	84.12	123.48	123.48
S/N F07	2.75	-0.50	0.05	3.19	76.52	109.29	111.63
S/N F13	2.78	0.14	-0.04	3.83	102.85	108.70	71.10
S/N F15	3.09	-0.14	-1.10	3.18	87.34	135.18	122.75
S/N F17	2.87	0.76	-0.09	2.81	119.53	120.55	80.32
Mean	2.88	0.02	-0.10	2.91	89.85	119.63	106.03
Std. Dev.	0.13	0.45	0.59	0.47	15.99	10.12	21.82

Table 2: Male Specimen Mass Properties

Male Specimens	Mass (kg)	CG <sub>x</sub> (cm)	CG <sub>y</sub> (cm)	CG <sub>z</sub> (cm)	MOI <sub>x</sub> (kg-cm <sup>2</sup> )	MOI <sub>y</sub> (kg-cm <sup>2</sup> )	MOI <sub>z</sub> (kg-cm <sup>2</sup> )
S/N M09	3.04	-0.11	-0.11	2.29	79.88	129.04	127.58
S/N M10	4.38	0.61	-0.19	2.11	145.43	223.26	223.50
S/N M11	3.53	-0.13	-0.48	2.76	162.40	164.45	110.46
S/N M12	3.96	0.10	-0.22	3.66	124.50	192.97	192.10
S/N M14	3.75	-0.15	0.39	2.25	117.63	174.54	177.03
S/N M18	3.21	0.33	0.34	1.57	142.65	148.64	99.78
S/N M19	2.92	0.17	-0.25	3.80	110.02	129.77	110.17
S/N M20	4.45	0.25	0.05	2.89	151.13	226.48	234.23
Mean	3.68	0.13	-0.06	2.84	129.20	173.64	160.61
Std. Dev.	0.53	0.27	0.30	0.76	26.68	38.27	55.86

Table 3: Overall Specimen Mass Properties

All Specimens	Mass (kg)	CG <sub>x</sub> (cm)	CG <sub>y</sub> (cm)	CG <sub>z</sub> (cm)	MOI <sub>x</sub> (kg-cm <sup>2</sup> )	MOI <sub>y</sub> (kg-cm <sup>2</sup> )	MOI <sub>z</sub> (kg-cm <sup>2</sup> )
Mean	3.27	0.08	-0.08	2.78	109.53	146.64	133.32
P. Std. Dev.	0.44	0.36	0.46	0.65	22.39	28.91	43.59

## CONCLUSIONS

The procedures used to conduct this study consisted of preparing the specimens, marking predetermined landmarks on the specimens' head and face, performing anthropometric measures on the specimen, dissecting the head from the neck, measuring the specimens' mass and CG with respect to a box coordinate system, measuring the specimens' principal moments of inertia with respect to the specimens' CG, digitizing appropriate landmarks on the box and specimens to transform the CG data from the box to the head anatomical coordinate system, performing the CT scans, analyzing the scans, calculating the mass properties of the specimens, and lastly, comparing the two sets of data (measured versus calculated).

The mass, centers of gravity, and principal moments of inertia were directly measured for 15 human cadaveric specimens. All computed tomographic scans were performed and are currently in the process of being analyzed to allow for the calculation of the specimen mass properties. Upon completion of this study, the two sets of data (measured *versus* calculated) will be statistically compared. Likewise, a comparison of these results with past studies will be performed for both mass properties and anthropometry.

It is the hope of these authors that this study will determine the efficacy of using electronic

imaging, specifically CT, to determine the mass properties of living human heads, and generate an additional useful set of human head mass properties and anthropometric data.

## REFERENCES

- BECKER, E. B., (1972). Measurement of Mass Distribution Parameters of Anatomical Segments. Proc. 16th Stapp Car Crash Conference, SAE Paper No. 720964, 81(4), pp. 2818-2833.
- BEIER, G., SCHULLER, E., SCHUCK, M., EWING, C.L., BECKER, E.D., and THOMAS, D.J., (1980). Center of Gravity and Moments of Inertia of Human Heads. Proc. 5<sup>th</sup> Int. IRCOBI Conference on the Biomechanics of Impact, p. 228.
- CHANDLER, R.F., CLAUSER, C.E., MCCONVILLE, J.T., REYNOLDS, H.M., and YOUNG, J.W., (1974). Investigation of Inertial Properties of The Human Body. AMRL-TR-74-137. Aerospace Medical Research Laboratory, Wright-Patterson AFB, Ohio.
- CLAUSER, C.E., MCCONVILLE, J.T., and YOUNG, J.W., (1969). Weight, Volume, and Center of Mass of Segments of The Human Body. AMRL-TR-69-70. Aerospace Medical Research Laboratory, Wright-Patterson AFB, Ohio.
- HARLESS, E., (1860). The Static Moments of The Component Masses of The Human Body. Trans. of the Math-Phys., Royal Bavarian Acad. of Sci., 8(1), pp. 69-96. Unpublished English Translation, FTD-TT-61-295, Wright-Patterson AFB, Ohio.
- KALEPS, I., CLAUSER, C.E., YOUNG, J.W., CHANDLER, R.F., ZEHNER, G.F., and MCCONVILLE, J.T., (1984). Investigation Into The Mass Distribution Properties of The Human Body and Its Segments. Ergonomics, 27(12), pp. 1225-1237.
- KNOX, F.S., III, BUHRMAN, J.R. and PERRY, C.E., (1992). Biomechanics of Ejection Safety For Night Vision Systems. Proc. Night Vision 92, London, U.K.
- MCCONVILLE, J.T., CHURCHILL, T.D., KALEPS, I., CLAUSER, C.E., and CUZZI, J., (1980). Anthropometric Relationships of Body and Body Segment Moment of Inertia. AFAMRL-TR-80-119. Air Force Aerospace Medical Research Laboratory, Wright-Patterson AFB, Ohio.
- SCHULTZ, R.B., OBERGEFELL, L.A., RIZER A.L., ALBERY, C.B., and ANDERSON, B.A., (1997). Comparison of Measured and Predicted Human Whole-Body Inertial Properties. Proc. 41st Stapp Car Crash Conference, SAE Paper No. 97S-57.
- SELF, B.P., SPITTLE, E.K., KALEPS, I., and ALBERY C.B., (1992). Accuracy and Repeatability of The Standard Automated Mass Properties Measurement System. AL-TR-1992-0137. Armstrong Laboratory, Wright-Patterson AFB, Ohio.
- WALKER, L.B., HARRIS, E.H., and PONTIUS, U.R., (1973). Mass, Volume, Center of Mass and Mass Moment of Inertia of Head and Head and Neck of Human Body. Final Report, AD 762 581. Dept. of Navy, Office of Naval Research, Washington, D.C.
- WHITESTONE, J.J., (2000). Estimation of Human Head Mass Properties Using CT Imaging: A proposal to AFRL/HEPA, March 3, 2000.
- WHITESTONE, J.J., and ALBERY, C.B., (1996). Assessment of The Hybrid II Manikin Headform as a Reference For Mass Properties Measurements of Helmet Systems. SAFE J., 26(3), pp. 9-17.